Delay Tolerant Cooperation in the Energy Harvesting Multiple Access Channel

Onur Kaya*, Nugman Su†, Sennur Ulukus‡, Mutlu Koca†
*Isik University, Istanbul, Turkey, onur.kaya@isikun.edu.tr
†Bogazici University, Istanbul, Turkey, {nugman.su,mutlu.koca}@boun.edu.tr
‡University of Maryland, College Park, MD, ulukus@umd.edu

***Abstract*—We consider the optimum transmit scheduling problem for a two user energy harvesting cooperative multiple access channel. We assume a slotted model where energy harvests in each slot are known a priori. We propose a delay tolerant cooperation model: the transmitters create common information in a given slot, but need not cooperatively send the created common information immediately; they may relegate all or part of the cooperative message transmission to upcoming slots. We propose a modified block Markov superposition coding scheme based on message re-partitioning, that spans multiple slots. We characterize the corresponding achievable departure region by a deadline, and maximize it subject to energy harvesting constraints. We show that, delay tolerant cooperation need not necessarily improve the departure region over delay constrained cooperation, and derive a sufficient condition for the equivalence of the two policies. We compare optimal delay constrained and delay tolerant cooperation policies, and their achievable departure regions via simulations.**

I. Introduction

Unlike traditional information theoretical models which impose average power constraints on transmissions, systems with nodes harvesting energy (solar, vibration absorbtion based etc.) from their environment have a real time peak energy constraint. In these setups, instantaneous lack of energy at the nodes may cause transmission outages. Therefore, the information theoretic encoding strategies based on random coding arguments do not immediately apply to energy harvesting models. Yet, it was recently shown in [1] that average power constrained capacity is still achievable under the more stringent energy harvesting constraints.

Once a rate-power relationship (i.e., capacity, achievable rate) for an energy harvesting communication model is established, one needs to determine how much of the available energy at each instant should be used immediately, and how much should be stored for later use. Motivated by this, several channel models, including point to point [2]–[5], broadcast [6]–[8], multiple access [9], [10], relay [11]–[13] and interference [14] channels have been revisited in the energy harvesting framework. In these works, transmission protocols that optimally use the harvested energy to minimize transmission completion time or to maximize the throughput by a deadline were obtained, under various assumptions on fading, battery size and energy/data arrival models. In this paper, we extend this optimization framework to the cooperative multiple access channel.

This work was supported by Tubitak Grant 113E556.

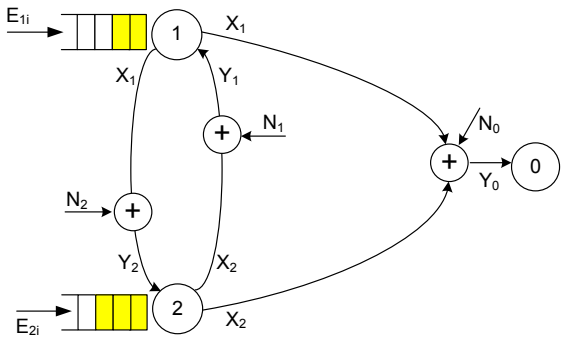

Fig. 1: Energy harvesting cooperative MAC model.

The cooperative multiple access channel, shown in Fig. 1, models bidirectional cooperation among energy harvesting nodes. The users over-hear each other's transmission, and can decode, re-encode and cooperatively send each other's data. This results in the well-known concept of user cooperation diversity [15]. However, under the energy harvesting framework, another type of diversity, namely *energy diversity* arises due to the variable nature of harvested energies. Hence, cooperation and transmit scheduling policies which take advantage of both forms of diversity need to be developed.

Recently, the transmit scheduling problem for the delay constrained energy harvesting cooperative multiple access channel was studied in [16], under the assumption that the common information created between two consecutive energy harvests must be immediately sent to the receiver within the same time-frame. The goal of this paper is to develop a new coding technique that alleviates this assumption and to investigate potential gains provided by the ability to delay the cooperative transmission of exchanged data, until the joint energy state of the users is more amenable to cooperation.

We first describe the message generation, encoding and decoding policies for the delay tolerant cooperation model, and characterize its achievable rates. Then, we state the departure region maximization problem for both delay constrained [16] and delay tolerant cooperation policies, and derive a sufficient condition for the equivalence of achievable departure regions. We demonstrate, through simulations, that while delay tolerant

cooperation does bring some improvement for cases with high variations in energy arrivals, this improvement is rather low, and is mostly one sided near one of the user rates. We observe that, in many cases the users procrastinate in cooperation: instead of establishing common information in early slots, they tend to save energy, and establish common information only when they need to cooperatively send it, effectively operating in a delay constrained mode even if they do not have to.

II. System Model

The energy harvesting cooperative multiple access channel consists of users 1, 2, communicating with each other and the receiver 0 over additive white Gaussian channels, as shown in Fig. 1. The received signals in slot i are given by,

$$\mathbf{Y}_{0i} = \mathbf{X}_{1i} + \mathbf{X}_{2i} + \mathbf{N}_{0i}, \tag{1}$$

$$\mathbf{Y}_{1i} = \mathbf{X}_{2i} + \mathbf{N}_{1i}, \tag{2}$$

$$\mathbf{Y}_{2i} = \mathbf{X}_{1i} + \mathbf{N}_{2i}, \tag{3}$$

where $\mathbf{X}_{ki}$ is the transmitted codeword by user k and $\mathbf{N}_{0i}$, $\mathbf{N}_{1i}$ and $\mathbf{N}_{2i}$ denote the additive white Gaussian noise (AWGN) terms at the respective nodes. The noise variance at the receiver is $\sigma^2 > 1$, while the noise variances at the users are assumed to be 1. The users harvest energy from their surroundings. The harvested energy is accumulated for T seconds in an unlimited sized battery, before being used for transmission. Therefore, we use an equivalent slotted energy arrival model where energy arrives in chunks every T seconds, and the arrivals occur just before the beginning of the next time slot of length T. We assume, without loss of generality, that there are a total of N slots, and the slot length is $T = 1$ seconds. The energy arrivals of users 1 and 2, right before time slot $i \in \{1, \dots, N\}$ are denoted by E_{1i} and E_{2i}, respectively.

III. Delay Constrained Cooperation

In this section, we review the delay constrained cooperation policy recently proposed in [16], as it will be used as a benchmark for the delay tolerant policy proposed in this paper.

In the delay constrained setup introduced in [16], the cooperation is carried out in a slot by slot basis: the common information established within a slot between two consecutive energy harvests is cooperatively conveyed in its entirety to the receiver, within the same slot. The users employ the block Markov encoding scheme of [15] in each slot, and the receiver employs backwards decoding at the end of each slot. The rates achievable in slot i can be characterized in terms of the transmit power variables as,

$$R_{1i} < \frac{1}{2}\log(1 + p_{12i}), \tag{4}$$

$$R_{2i} < \frac{1}{2}\log(1 + p_{21i}), \tag{5}$$

$$R_{1i} + R_{2i} < \frac{1}{2}\log\Big(\frac{S_i}{\sigma^2}\Big), \tag{6}$$

where $S_i \triangleq \sigma^2 + p_{1i} + p_{2i} + 2\sqrt{p_{U_1 i} p_{U_2 i}}$; p_{12i} and p_{21i} are sub-powers used to create common information, $p_{U_1 i}$ and $p_{U_2 i}$ are sub-powers used to convey common information to the receiver, and p_{1i} and p_{2i} are the total powers used by users 1 and 2, respectively. Although the cooperation in each slot is carried out independently of the remaining slots, the achievable rates in each slot are inherently coupled, since the transmissions are subject to cumulative energy constraints spanning multiple slots:

$$\sum_{i=1}^{\ell} p_{12i} + p_{U_1 i} \triangleq \sum_{i=1}^{\ell} p_{1i} \leq \sum_{i=1}^{\ell} E_{1i}, \quad \ell = 1, \dots, N, \tag{7}$$

$$\sum_{i=1}^{\ell} p_{21i} + p_{U_2 i} \triangleq \sum_{i=1}^{\ell} p_{2i} \leq \sum_{i=1}^{\ell} E_{2i}, \quad \ell = 1, \dots, N. \tag{8}$$

Denoting the total number of bits departed by user k by $B_k = \sum_i R_{ki}$, the achievable departure region is defined as the set of $\{B_1, B_2\}$ pairs that are achievable under the rate and energy causality constraints. An algorithm that can be used to maximize this departure region was given in [16].

The main motivation of this paper is to investigate possible gains obtainable by removing the delay constraint from the encoding and decoding schemes in [16]. In what follows, we propose a delay tolerant achievability scheme, and derive its achievable departure region.

IV. Delay Tolerant Achievability Scheme

A. Message Generation

Users 1 and 2 aim to convey their independent messages $w_1 \in \{1, \dots, 2^{nNR_1}\}$ and $w_2 \in \{1, \dots, 2^{nNR_2}\}$, respectively, to the receiver. They partition these messages into N sub-messages each, $w_{1i} \in \{1, \dots, 2^{nR'_{1i}}\}$ and $w_{2i} \in \{1, \dots, 2^{nR'_{2i}}\}$, respectively, to be sent in time-slot $i = 1, \dots, N$. In the encoding, sub-messages from these alphabets will be transmitted B times per slot, to enable block Markov encoding. Hence we index the sub-messages by block index b, for $b = 1, \dots, B$, giving $w_{1i}(b) \in \{1, \dots, 2^{nR'_{1i}}\}$ and $w_{2i}(b) \in \{1, \dots, 2^{nR'_{2i}}\}$. Note that, by design, the sub-messages $w_{ki}(b)$, $b = 1, \dots, B$ belonging to the same slot i are all drawn from the same alphabet, hence they have the same rate R'_{ki}. Clearly $\sum_{i=1}^{N} R'_{ki} = NR_k$.

The users further re-partition their messages w_1 and w_2 into N sub messages each, $v_{1i} \in \{1, \dots, 2^{nR_{1i}}\}$ and $v_{2i} \in \{1, \dots, 2^{nR_{2i}}\}$, where $\sum_{i=1}^{\ell} R_{1i} \leq \sum_{i=1}^{\ell} R'_{1i}$ and $\sum_{i=1}^{\ell} R_{2i} \leq \sum_{i=1}^{\ell} R'_{2i}$, $\forall \ell = 1, \dots, N$. Again, in encoding, these alphabets will be used B times per slot, hence the notation $v_{1i}(b) \in \{1, \dots, 2^{nR_{1i}}\}$, $v_{2i}(b) \in \{1, \dots, 2^{nR_{2i}}\}$ will be used from now on. The partitioning is carried out as follows: starting with slot $i = 1$, each $w_{1i}(b)$ is divided into two components: $w_{1i}(b) = \{v_{1i}(b), z_{1i}(b)\}$. The *leftover* message $z_{1i}(b)$ in slot i, block b, is merged with the message $w_{1(i+1)}(b)$ in the same block of the next slot, and then re-partitioned as $\{w_{1(i+1)}(b), z_{1i}(b)\} = \{v_{1(i+1)}(b), z_{1(i+1)}(b)\}$. This continues until all messages $w_{1i}(b)$, are re-partitioned into $v_{1i}(b)$. The same process is repeated for user 2. Clearly $\sum_{i=1}^{N} R_{ki} = NR_k$. Since the time slots are assumed to be unit length, the total departure of user k can be expressed as $B_k = \sum_{i=1}^{N} R_{ki}$. Without loss of generality, we carry out

our analysis throughout the paper with rates expressed in bits per channel use, until the simulation results section where we convert them to bits/sec under a given bandwidth limitation.

B. Codebook Generation

The codebook generation proceeds as follows.

- Generate, $\forall i$, $2^{n(R_{12i}+R_{21i})}$ length-n sequences $\mathbf{u}_i$, and map them to distinct message pairs $\{v_{1i}, v_{2i}\}$, forming $\mathbf{u}_i(v_{1i}, v_{2i})$.
- Generate, $\forall i$ and $\forall \mathbf{u}_i(v_{1i}, v_{2i})$, $2^{nR'_{12i}}$ length-n codewords $\mathbf{x}_{12i}$, and map them to distinct messages w_{1i}, forming $\mathbf{x}_{12i}(w_{1i}, v_{1i}, v_{2i})$.
- Generate, $\forall i$ and $\forall \mathbf{u}_i(v_{1i}, v_{2i})$, $2^{nR'_{21i}}$ length-n codewords $\mathbf{x}_{21i}$, and map them to distinct messages w_{2i}, forming $\mathbf{x}_{21i}(w_{2i}, v_{1i}, v_{2i})$.

C. Encoding and Decoding

In each slot, each user accesses the channel nB times, where $n, B \to \infty$. User k selects a message w_k, and partitions it as described in message generation section. For the encoding to start in the first block $b = 1$ of each slot i, $(v_{ki}(0), v_{ji}(0))$ is arbitrarily set to (1,1).

In each slot i, block b, user k selects the codewords $\mathbf{x}_{kji}(b) \triangleq \mathbf{x}_{kji}(w_{ki}(b), v_{ki}(b-1), v_{ji}(b-1))$ and $\mathbf{u}_i(b) \triangleq \mathbf{u}_i(v_{ki}(b-1), v_{ji}(b-1))$, superposes them and sends them to its cooperating partner and the receiver. Letting $\mathbf{X}_{kji} = [\mathbf{x}_{kji}(1), \ldots, \mathbf{x}_{kji}(B)]$ and $\mathbf{U}_i = [\mathbf{u}_i(1), \ldots, \mathbf{u}_i(B)]$, the transmitted codewords by the users over each slot i can be written concisely as,

$$\mathbf{X}_{1i} = \sqrt{p_{12i}}\mathbf{X}_{12i} + \sqrt{p_{U_1i}}\mathbf{U}_i, \quad i = 1, \ldots, N, \tag{9}$$

$$\mathbf{X}_{2i} = \sqrt{p_{21i}}\mathbf{X}_{21i} + \sqrt{p_{U_2i}}\mathbf{U}_i, \quad i = 1, \ldots, N, \tag{10}$$

where the powers p_{kji} and p_{U_ki} satisfy the same energy causality constraints (7)-(8) as in the delay constrained scenario.

The decoding at the cooperating partner is carried out at the end of each block of each slot. At the beginning of block b, users k and j will have decoded the messages $w_{ji}(b-1)$ and $w_{ki}(b-1)$, and therefore can form both of $v_{ji}(b-1)$ and $v_{ki}(b-1)$. The same encoding procedure can now be carried out, sequentially in the next slots. In the last block $b = B$ of each slot i, $(w_{ki}(0), w_{ji}(0))$ is arbitrarily set to (1,1).

The decoding at the receiver is performed in the backward direction, starting with $i = N$, $b = B$. Since there is no fresh information transmission in the very last block, the receiver uses the received signal to decode $v_{kN}(B-1), v_{jN}(B-1)$, using joint typicality check. Due to the structure of the message generation process, $\{z_{kN}(b), z_{jN}(b)\} = \emptyset$, $\forall b$ in the last slot, and the messages $v_{kN}(B-1), v_{jN}(B-1)$ have necessarily higher rates than $w_{kN}(B-1), w_{jN}(B-1)$. In fact, $w_{kN}(B-1), w_{jN}(B-1)$, as well as $z_{k(N-1)}(B-1), z_{j(N-1)}(B-1)$ can be uniquely determined from $v_{kN}(B-1), v_{jN}(B-1)$, in block B. Therefore, the decoding may now move to block $B-1$, and the receiver decodes $v_{kN}(B-2), v_{jN}(B-2)$, and hence, $w_{kN}(B-2), w_{jN}(B-2)$. The same backward decoding procedure is repeated for all blocks in slot N until block 1. At this point, the receiver has decoded all information that was exchanged in the last slot, and some accumulated information, $z_{k(N-1)}(b), z_{j(N-1)}(b)$ that was exchanged in the previous slots. The decoding then moves to slot $N-1$. Since $z_{k(N-1)}(b), z_{j(N-1)}(b)$ is already known, decoding $v_{k(N-1)}(b), v_{j(N-1)}(b)$ is equivalent to decoding $w_{k(N-1)}(b), w_{j(N-1)}(b)$. Repeating this process until all slots are decoded, yields w_1 and w_2.

D. Achievable Rates

In each slot i, the decoding at each user k is equivalent to single user decoding of message w_{ji} from the received $\mathbf{X}_{ji}$. Error free decoding of w_{ji} is possible if

$$R'_{1i} \leq \frac{1}{2}\log(1 + p_{12i}), \tag{11}$$

$$R'_{2i} \leq \frac{1}{2}\log(1 + p_{21i}). \tag{12}$$

On the other hand, for error free decoding of v_{ki}, v_{ji} at the receiver in slot i, we need,

$$R_{1i} + R_{2i} \leq \frac{1}{2}\log\Big(\frac{S_i}{\sigma^2}\Big). \tag{13}$$

The crucial observation here is that these rate constraints are over different rate variables by design, however these variables are related as follows:

$$\sum_{i=1}^{\ell} R_{1i} \leq \sum_{i=1}^{\ell} R'_{1i}, \qquad \ell = 1, \ldots, N \tag{14}$$

$$\sum_{i=1}^{\ell} R_{2i} \leq \sum_{i=1}^{\ell} R'_{2i}, \qquad \ell = 1, \ldots, N \tag{15}$$

$$\sum_{i=1}^{N} R_{1i} = \sum_{i=1}^{N} R'_{1i} = NR_1 \tag{16}$$

$$\sum_{i=1}^{N} R_{2i} = \sum_{i=1}^{N} R'_{2i} = NR_2 \tag{17}$$

We will now get rid of the auxiliary rate variables R'_{2i}, which can be viewed as the rates at which the common information is generated, and characterize the bounds on per slot achievable rates.

Lemma 1 *The constraints in* (11) *and* (12) *must be satisfied with equality, i.e.,*

$$R'_{1i} = \frac{1}{2}\log(1 + p_{12i}), \tag{18}$$

$$R'_{2i} = \frac{1}{2}\log(1 + p_{21i}). \tag{19}$$

Proof: The proof follows by noting that, if (11) is loose, there exists a strictly better policy which uses less power p_{12i}, yet achieves the same rate. Same argument holds for (12). ■

Using (18) and (19) in (14) and (15), we get the following set of achievable rates:

$$\sum_{i=1}^{\ell} R_{1i} \leq \sum_{i=1}^{\ell} \frac{1}{2}\log(1 + p_{12i}), \qquad \ell = 1, \ldots, N \tag{20}$$

$$\sum_{i=1}^{\ell} R_{2i} \leq \sum_{i=1}^{\ell} \frac{1}{2}\log(1+p_{21i}), \qquad \ell = 1,\ldots,N \quad (21)$$

$$R_{1i} + R_{2i} \leq \frac{1}{2}\log\left(\frac{S_i}{\sigma^2}\right), \qquad i = 1,\ldots,N \quad (22)$$

Comparing (20)-(22) to (4)-(6), it is evident that the former set is in general looser, as we have cumulative constraints on rates rather than per slot constraints. The sum rate constraint however is identical for both delay constrained and delay tolerant cooperation. In the next section, we will state the departure region maximization problem for both techniques, derive necessary and sufficient conditions for optimality, and show that the achievable departure region of the two techniques may be identical under some conditions.

V. Departure Region Maximization

The departure region for the energy harvesting cooperative MAC is convex, because of the possibility of time-sharing. Therefore, it can be optimized in the delay non-constrained framework by maximizing a weighted sum of rates, for some weights $\{\mu_1, \mu_2\}$:

$\mathbf{P1}$:

$$\max_{\mathbf{p}, R_{1i}, R_{2i}} \mu_1 \sum_{i=1}^{N} R_{1i} + \mu_2 \sum_{i=1}^{N} R_{2i} \quad (23)$$

$$\text{s.t.} \sum_{i=1}^{\ell} p_{12i} + p_{U_1 i} \leq \sum_{i=1}^{\ell} E_{1i}, \quad \ell = 1,\ldots,N, \quad (24)$$

$$\sum_{i=1}^{\ell} p_{21i} + p_{U_2 i} \leq \sum_{i=1}^{\ell} E_{2i}, \quad \ell = 1,\ldots,N, \quad (25)$$

$$\sum_{i=1}^{\ell} R_{1i} \leq \sum_{i=1}^{\ell} \frac{1}{2}\log(1+p_{12i}), \quad \ell = 1,\ldots,N, \quad (26)$$

$$\sum_{i=1}^{\ell} R_{2i} \leq \sum_{i=1}^{\ell} \frac{1}{2}\log(1+p_{21i}), \quad \ell = 1,\ldots,N, \quad (27)$$

$$R_{1i} + R_{2i} \leq \frac{1}{2}\log\left(\frac{S_i}{\sigma^2}\right), \quad i = 1,\ldots,N, \quad (28)$$

$$p_{12i}, p_{U_1 i}, p_{21i}, p_{U_2 i} \geq 0, \quad i = 1,\ldots,N, \quad (29)$$

$$R_{1i}, R_{2i} \geq 0, \qquad i = 1,\ldots,N. \quad (30)$$

Likewise, the achievable departure region for the delay constrained model can be obtained by solving a similar optimization problem, if (26) and (27) are replaced with (34) and (35), respectively:

$\mathbf{P2}$:

$$\max_{\mathbf{p}, R_{1i}, R_{2i}} \mu_1 \sum_{i=1}^{N} R_{1i} + \mu_2 \sum_{i=1}^{N} R_{2i} \quad (31)$$

$$\text{s.t.} \sum_{i=1}^{\ell} p_{12i} + p_{U_1 i} \leq \sum_{i=1}^{\ell} E_{1i}, \quad \ell = 1,\ldots,N, \quad (32)$$

$$\sum_{i=1}^{\ell} p_{21i} + p_{U_2 i} \leq \sum_{i=1}^{\ell} E_{2i}, \quad \ell = 1,\ldots,N, \quad (33)$$

$$R_{1i} \leq \frac{1}{2}\log(1+p_{12i}), \quad i = 1,\ldots,N, \quad (34)$$

$$R_{2i} \leq \frac{1}{2}\log(1+p_{21i}), \quad i = 1,\ldots,N, \quad (35)$$

$$R_{1i} + R_{2i} \leq \frac{1}{2}\log\left(\frac{S_i}{\sigma^2}\right), \quad i = 1,\ldots,N, \quad (36)$$

$$p_{12i}, p_{U_1 i}, p_{21i}, p_{U_2 i} \geq 0, \quad i = 1,\ldots,N, \quad (37)$$

$$R_{1i}, R_{2i} \geq 0, \qquad i = 1,\ldots,N. \quad (38)$$

Now, we will show that, delay tolerant cooperation for the energy harvesting cooperative MAC need not necessarily yield better departure region compared to its delay constrained counterpart.

Theorem 1 *Let the optimal rate allocation which solves problem* $\mathbf{P2}$ *for weights* μ_1 *and* μ_2 *satisfy* $R_{1i}^* > 0$ *and* $R_{2i}^* > 0$ $\forall i$. *Then* R_{1i}^* *and* R_{2i}^* *are also the solution for* $\mathbf{P1}$, *and the optimal power allocation policies under the delay constrained and tolerant setups are identical.*

Proof: We will prove the theorem by showing that the KKT conditions for both problems become identical, under the condition $R_{1i}^* > 0$ and $R_{2i}^* > 0$ $\forall i$. Associating non-negative Lagrange multipliers for each inequality constraint, we obtain the Lagrangian for the convex problem given in (23)-(30) as

$$\begin{aligned} L = &\sum_{i=1}^{N} [\mu_1 R_{1i} + \mu_2 R_{2i}] \\ &+ \sum_{\ell=1}^{N} \gamma_{1\ell} \sum_{i=1}^{\ell} \left[\frac{1}{2}\log(1+p_{12i}) - R_{1i}\right] \\ &+ \sum_{\ell=1}^{N} \gamma_{2\ell} \sum_{i=1}^{\ell} \left[\frac{1}{2}\log(1+p_{21i}) - R_{2i}\right] \\ &+ \sum_{i=1}^{N} \gamma_{si} \left[\frac{1}{2}\log\left(\frac{S_i}{\sigma^2}\right) - R_{1i} - R_{2i}\right] \\ &+ \sum_{\ell=1}^{N} \lambda_{1\ell} \left[\sum_{i=1}^{\ell} E_{1i} - p_{12i} - p_{U_1 i}\right] \\ &+ \sum_{\ell=1}^{N} \lambda_{2\ell} \left[\sum_{i=1}^{\ell} E_{2i} - p_{21i} - p_{U_2 i}\right] \\ &+ \sum_{i=1}^{N} [\xi_{12i} p_{12i} + \xi_{21i} p_{21i} + \xi_{U_1 i} p_{U_1 i} + \xi_{U_2 i} p_{U_2 i}] \\ &+ \sum_{i=1}^{N} [\xi_{R_1 i} R_{1i} + \xi_{R_2 i} R_{2i}] \end{aligned} \quad (39)$$

Taking the partial derivatives of the Lagrangian, and imposing the complementary slackness conditions, we get the following KKT conditions, for $i = 1,\ldots,N$:

$$\mu_1 - \sum_{\ell=i}^{N} \gamma_{1\ell} - \gamma_{si} + \xi_{R_1 i} = 0 \quad (40)$$

$$\mu_2 - \sum_{\ell=i}^{N} \gamma_{2\ell} - \gamma_{si} + \xi_{R_2 i} = 0 \quad (41)$$

$$\frac{1}{2}\left(\frac{\sum_{\ell=i}^{N}\gamma_{1\ell}}{1+p_{12i}} + \frac{\gamma_{si}}{S_i}\right) - \sum_{\ell=i}^{N}\lambda_{1\ell} + \xi_{12i} = 0 \quad (42)$$

$$\frac{1}{2}\left(\frac{\sum_{\ell=i}^{N}\gamma_{2\ell}}{1+p_{21i}} + \frac{\gamma_{si}}{S_i}\right) - \sum_{\ell=i}^{N}\lambda_{2\ell} + \xi_{21i} = 0 \quad (43)$$

$$\frac{\gamma_{si}}{2}\frac{1+\sqrt{\frac{p_{U_2 i}}{p_{U_1 i}}}}{S_i} - \sum_{\ell=i}^{N}\lambda_{1\ell} + \xi_{U_1 i} = 0 \quad (44)$$

$$\frac{\gamma_{si}}{2}\frac{1+\sqrt{\frac{p_{U_1 i}}{p_{U_2 i}}}}{S_i} - \sum_{\ell=i}^{N}\lambda_{2\ell} + \xi_{U_2 i} = 0 \quad (45)$$

$$\xi_{12i}p_{12i} = \xi_{21i}p_{21i} = \xi_{U_1 i}p_{U_1 i} = \xi_{U_2 i}p_{U_2 i} = 0 \quad (46)$$

$$\xi_{R_1 i}R_{1i} = \xi_{R_2 i}R_{2i} = 0. \quad (47)$$

The jointly optimum delay tolerant transmit scheduling and cooperation policy can be obtained by solving (40)-(47), together with the primal feasibility conditions (24)-(30).

Similarly, it is easy to show that the KKT conditions for **P2** are

$$\mu_1 - \gamma_{1i} - \gamma_{si} + \xi_{R_1 i} = 0 \quad (48)$$

$$\mu_2 - \gamma_{2i} - \gamma_{si} + \xi_{R_2 i} = 0 \quad (49)$$

$$\frac{1}{2}\left(\frac{\gamma_{1i}}{1+p_{12i}} + \frac{\gamma_{si}}{S_i}\right) - \sum_{\ell=i}^{N}\lambda_{1\ell} + \xi_{12i} = 0 \quad (50)$$

$$\frac{1}{2}\left(\frac{\gamma_{2i}}{1+p_{21i}} + \frac{\gamma_{si}}{S_i}\right) - \sum_{\ell=i}^{N}\lambda_{2\ell} + \xi_{21i} = 0 \quad (51)$$

$$\frac{\gamma_{si}}{2}\frac{1+\sqrt{\frac{p_{U_2 i}}{p_{U_1 i}}}}{S_i} - \sum_{\ell=i}^{N}\lambda_{1\ell} + \xi_{U_1 i} = 0 \quad (52)$$

$$\frac{\gamma_{si}}{2}\frac{1+\sqrt{\frac{p_{U_1 i}}{p_{U_2 i}}}}{S_i} - \sum_{\ell=i}^{N}\lambda_{2\ell} + \xi_{U_2 i} = 0 \quad (53)$$

$$\xi_{12i}p_{12i} = \xi_{21i}p_{21i} = \xi_{U_1 i}p_{U_1 i} = \xi_{U_2 i}p_{U_2 i} = 0 \quad (54)$$

$$\xi_{R_1 i}R_{1i} = \xi_{R_2 i}R_{2i} = 0, \quad (55)$$

in conjunction with the primal feasibility conditions (32)-(38).

The KKT conditions (52)-(55) are identical to (44)-(47). Therefore, it suffices to show that the remaining KKT conditions overlap, and the primal feasibility constraints are satisfied for both problems. To this end, let $R_{1i}^* > 0$ and $R_{2i}^* > 0$, $i = 1, \ldots, N$, be a solution to **P2**, for given μ_1 and μ_2. Then, by (55), $\xi_{R_1 i} = \xi_{R_2 i} = 0$ and (48) and (49) yield

$$\gamma_{1i} = \mu_1 - \gamma_{si}, \qquad \forall i \quad (56)$$

$$\gamma_{2i} = \mu_2 - \gamma_{si}, \qquad \forall i. \quad (57)$$

Substituting these in (50) and (51), the dependence of the conditions on γ_{1i} and γ_{2i} can be dropped:

$$\frac{1}{2}\left(\frac{\mu_1 - \gamma_{si}}{1+p_{12i}} + \frac{\gamma_{si}}{S_i}\right) - \sum_{\ell=i}^{N}\lambda_{1\ell} + \xi_{12i} = 0 \quad (58)$$

$$\frac{1}{2}\left(\frac{\mu_2 - \gamma_{si}}{1+p_{21i}} + \frac{\gamma_{si}}{S_i}\right) - \sum_{\ell=i}^{N}\lambda_{2\ell} + \xi_{21i} = 0. \quad (59)$$

We will now show that the positive per slot rates $R_{1i}^* > 0$ and $R_{2i}^* > 0$ that solve **P2** also satisfy the KKT conditions for **P1**. Substituting these rates in (47), $\xi_{R_1 i} = \xi_{R_2 i} = 0$, and (40) and (41) yield

$$\sum_{\ell=i}^{N}\gamma_{1\ell} = \mu_1 - \gamma_{si}, \qquad \forall i \quad (60)$$

$$\sum_{\ell=i}^{N}\gamma_{2\ell} = \mu_2 - \gamma_{si}, \qquad \forall i. \quad (61)$$

Using these, (42) and (43) become identical to (58) and (59), obtained in the delay constrained case. Finally, since any solution that satisfies the primal feasibility conditions (34)-(35) is guaranteed to satisfy the looser primal feasibility conditions (26)-(27) for the delay tolerant case, the positive rates satisfying the KKT conditions for the delay constrained problem, and the corresponding powers that achieve them, also satisfy the KKT conditions for the delay tolerant problem, thereby completing the proof. ■

In the following section, we provide some simulation results demonstrating that the condition derived in Theorem 1 is satisfied quite frequently, and the less complex delay constrained cooperation may indeed achieve the same departure region as the delay tolerant cooperation. We also demonstrate some scenarios where delay tolerant cooperation performs better, especially near the single user rate point.

VI. Simulation Results

In this section, we evaluate the departure region of the proposed delay tolerant cooperation strategy for the energy harvesting MAC, and compare it to delay constrained cooperation from [16]. To simulate asymmetrical energy arrival patterns, as well as time variation of energy, we employ a doubly randomized model, where the components of the energy arrival vectors of each user are selected from independent uniform distributions in (0,20), and each of these vectors are then further multiplied by independent uniform random variables taking values in (0,1). The noise variance on the direct links is selected as $\sigma^2 = 2$, while the inter-user link noise variances are set to unity. The number of bits departed by user k is computed by first expressing the rates in terms of bits/sec, and then summing them over the transmission duration. Hence, the departure of each user is computed using $B_k = \sum_{i=1}^{N} W \log(1+p_{kji})$, where W is the system bandwidth. In the simulations, we assume that $W = 1$ MHz.

Of the 400 simulations performed with random energy arrival patterns with length $N = 4$, roughly 50% resulted in identical departure regions for the delay tolerant and delay constrained cooperation models, verifying Theorem 1. When the departure regions differ, the gain from delay tolerance was mostly one sided and maximum improvement was observed at the single user rate. In cases where delay tolerant cooperation

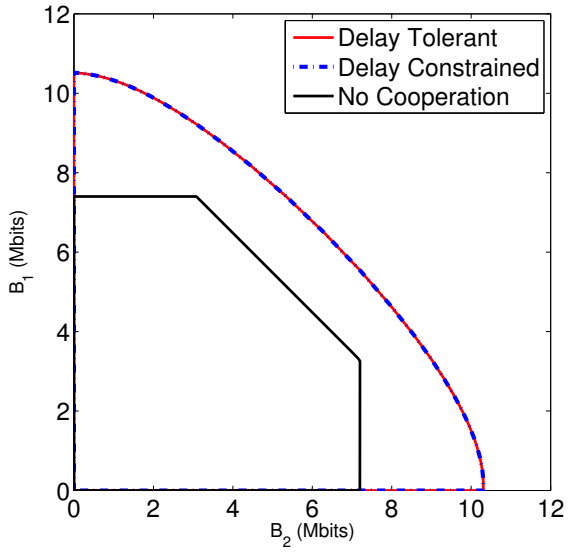

Fig. 2: Achievable departure regions for delay tolerant and delay constrained cooperation vs. non-cooperative MAC for $E_1 = [9.11,\ 1.83,\ 2.60,\ 7.78]$ and $E_2 = [10.35,\ 5.33,\ 3.68,\ 0.50]$.

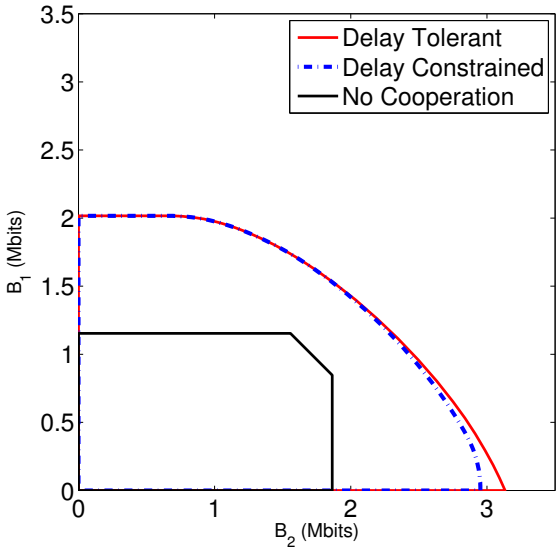

Fig. 3: Achievable departure regions for delay tolerant and delay constrained cooperation vs. non-cooperative MAC for $E_1 = [0.02,\ 0.40,\ 0.25,\ 1.26]$ and $E_2 = [0.65,\ 0.71,\ 0.73,\ 0.97]$.

performed better, it was observed that for at least one slot, one of the users received a very low energy level, and its resulting rate for that slot was 0. Among all simulations performed, the average improvement in the single user rate delay tolerant cooperation brings over delay constrained cooperation was less than 0.5%.

In Fig. 2, we demonstrate a case with $E_1 = [9.11,\ 1.83,\ 2.60,\ 7.78]$ and $E_2 = [10.35,\ 5.33,\ 3.68,\ 0.50]$, where the delay constrained and delay tolerant departure regions overlap. The power allocation policies for the two models are identical. In Fig. 3, we demonstrate a case where delay tolerant cooperation results in a better departure region. The energy arrivals resulting in Fig. 3 are $E_1 = [0.02,\ 0.40,\ 0.25,\ 1.26]$ and $E_2 = [0.65,\ 0.71,\ 0.73,\ 0.97]$. In what follows, we investigate the power and rate allocation policies for the delay constrained and delay tolerant cooperation models, for the maximum throughput and for maximum B_2 point in Fig. 3, in detail.

The power and rate allocation policies that maximize the total throughput for the delay constrained setup, obtained by setting $\mu_1 = \mu_2 = 1$ in **P2** are depicted in Fig. 4. The breakdown of cooperative powers show that in the first slot, user 1 uses all of its power to relay the signal of user 2. This is also reflected on the per-slot rates: user 1 gets zero rate in slot 1. Note that, the resulting rate allocation does not obey the hypothesis of Theorem 1, therefore this case is a candidate for possible discrepancy among the delay constrained and delay tolerant performance. The curves labelled "transmission rate" and "decoding rate" refer to the rates at which common information is created at the cooperative partner, and decoded at the receiver, respectively, in each slot. These rates are identical in the delay constrained setup, see [16].

The power and rate allocation policies that maximize the total throughput for the delay tolerant setup, obtained by setting $\mu_1 = \mu_2 = 1$ in **P1** are depicted in Fig. 5. Note that, user 1 still does not transmit its own data in slot 1, and its power allocation policy has changed slightly. However, user 2 uses much more of this power to send its own data in the first slot, as now the created common information need not be fully sent. The transmission rates, i.e., R'_{1i} and R'_{2i}, are initially higher than the decoding rates, R_{1i} and R_{2i}, thereby actively taking advantage of delay tolerance. However, these rates catch up as transmission progresses, as expected.

A similar analysis is carried out for the single user point in Fig. 3 on the B_2 axis ($\mu_1 = 0$, $\mu_2 = 1$). The results are depicted in Figs. 6 and 7. In this case, user 1 is expected to act as a dedicated relay for user 2, hence p_{12i} should be set to 0 in all slots. Note that, this seems to contradict user 1's power allocation in Fig. 6 for the delay constrained case, as user 1 uses a non-negative power for its own transmission in the last slot and as a result, sends a message at a non-zero rate, which is not meant to be decoded. However, note that the optimal policy for user 2 in the last slot is to only send its own signal; $p_{U_24} = 0$ and there is no coherent combining in the last slot. Therefore, user 1's energy in the last slot is wasted, as it has already transmitted all the cooperative information created by user 2. This leads to a non-unique solution in the last slot, and p_{124} is set to an arbitrary value. Note that, user 1 not being able to use all of its energy for cooperation is due to the delay constraint: energy received in the last slot cannot be used to convey earlier data. We observe that delay tolerant cooperation speeds up user 2's transmissions in earlier slots,

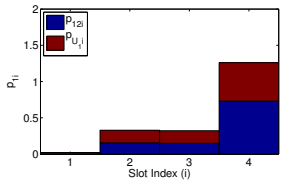

(a) User 1 power breakdown.

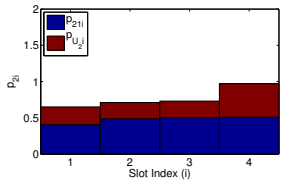

(b) User 2 power breakdown.

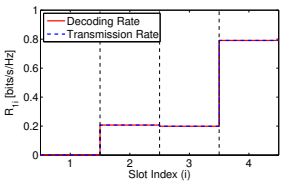

(c) User 1 rate allocation.

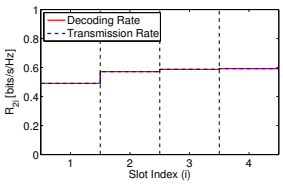

(d) User 2 rate allocation.

Fig. 4: Throughput optimal rate and power allocation in delay constrained setup.

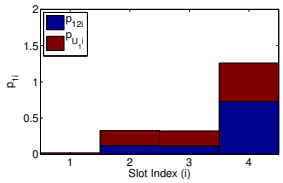

(a) User 1 power breakdown.

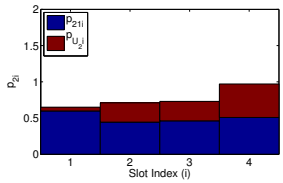

(b) User 2 power breakdown.

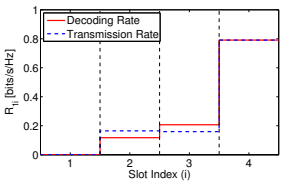

(c) User 1 rate allocation.

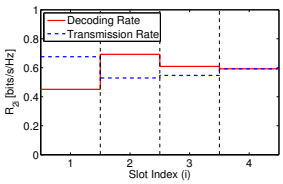

(d) User 2 rate allocation.

Fig. 5: Throughput optimal rate and power allocation in delay tolerant setup.

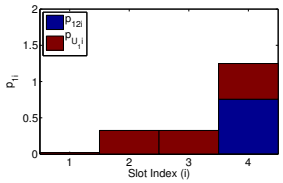

(a) User 1 power breakdown.

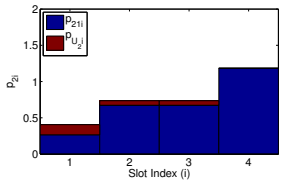

(b) User 2 power breakdown.

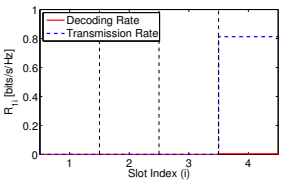

(c) User 1 rate allocation.

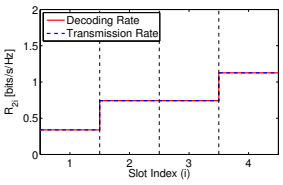

(d) User 2 rate allocation.

Fig. 6: B_2 maximizing rate and power allocation in delay constrained setup.

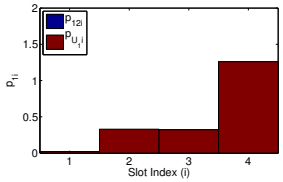

(a) User 1 power breakdown.

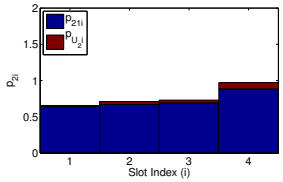

(b) User 2 power breakdown.

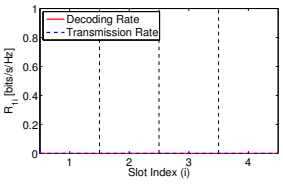

(c) User 1 rate allocation.

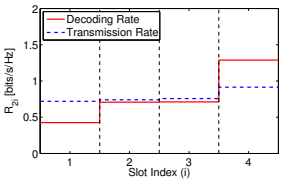

(d) User 2 rate allocation.

Fig. 7: B_2 maximizing rate and power allocation in delay tolerant setup.

uses all of user 1's energy, and achieves a higher rate.

VII. Conclusion

In this paper, we proposed a delay tolerant encoding and decoding model for the cooperative MAC. We characterized the departure region of the system, and compared it with that of delay constrained cooperation. While the departure region of the proposed delay tolerant cooperation model is potentially larger in general, simulation results show that the regions for delay constrained and tolerant policies either overlap, or differ by a small amount. This points to the interesting observation that the users can get near-delay tolerant performance if they procrastinate in cooperation; that is, if, instead of forming common information ahead of time, they save their energy and perform delay constrained cooperation in future slots. This demonstrates that, the potential flow of energy to future slots, which is already incorporated into delay constrained cooperation, is often sufficient to take advantage of the energy diversity, and further diversification of transmission rates by means of delaying transmissions is often not required.

References

[1] O. Ozel and S. Ulukus, "Achieving AWGN capacity under stochastic energy harvesting," *IEEE Trans. Inf. Theory*, vol. 58, no. 10, pp. 6471–6483, Oct. 2012.

[2] J. Yang and S. Ulukus, "Optimal packet scheduling in an energy harvesting communication system," *IEEE Trans. Commun.*, vol. 60, no. 1, pp. 220–230, Jan. 2012.

[3] K. Tutuncuoglu and A. Yener, "Optimum transmission policies for battery limited energy harvesting nodes," *IEEE Trans. Wireless Commun.*, vol. 11, no. 3, pp. 1180–1189, Mar. 2012.

[4] O. Ozel, K. Tutuncuoglu, J. Yang, S. Ulukus, and A. Yener, "Transmission with energy harvesting nodes in fading wireless channels: Optimal policies," *IEEE J. Sel. Areas Commun.*, vol. 29, no. 8, pp. 1732–1743, Sep. 2011.

[5] C. K. Ho and R. Zhang, "Optimal energy allocation for wireless communications with energy harvesting constraints," *IEEE Trans. Signal Process.*, vol. 60, no. 9, pp. 4808–4818, Sep. 2012.

[6] J. Yang, O. Ozel, and S. Ulukus, "Broadcasting with an energy harvesting rechargeable transmitter," *IEEE Trans. Wireless Commun.*, vol. 11, no. 2, pp. 571–583, Feb. 2012.

[7] M. A. Antepli, E. Uysal-Biyikoglu, and H. Erkal, "Optimal packet scheduling on an energy harvesting broadcast link," *IEEE J. Sel. Areas Commun.*, vol. 29, no. 8, pp. 1721–1731, Sep. 2011.

[8] O. Ozel, J. Yang, and S. Ulukus, "Optimal broadcast scheduling for an energy harvesting rechargeable transmitter with a finite capacity battery," *IEEE Trans. Wireless Commun.*, vol. 11, no. 6, pp. 2193–2203, Jun. 2012.

[9] J. Yang and S. Ulukus, "Optimal packet scheduling in a multiple access channel with energy harvesting transmitters," *Journal of Communications and Networks*, vol. 14, no. 2, pp. 140–150, Apr. 2012.

[10] Z. Wang, V. Aggarwal, and X. Wang, "Iterative dynamic water-filling for fading multiple-access channels with energy harvesting," *IEEE J. Sel. Areas Commun.*, vol. 33, no. 3, pp. 382–395, Mar. 2015.

[11] D. Gunduz and B. Devillers, "Two-hop communication with energy harvesting," in *4th IEEE CAMSAP*, Dec. 2011.

[12] C. Huang, R. Zhang, and S. Cui, "Throughput maximization for the gaussian relay channel with energy harvesting constraints," *IEEE J. Sel. Areas Commun.*, vol. 31, no. 8, pp. 1469–1479, Aug. 2013.

[13] Y. Luo, J. Zhang, and K. B. Letaief, "Optimal scheduling and power allocation for two-hop energy harvesting communication systems," *IEEE Trans. Wireless Commun.*, vol. 12, no. 9, pp. 4729–4741, Sep. 2013.

[14] K. Tutuncuoglu and A. Yener, "Sum-rate optimal power policies for energy harvesting transmitters in an interference channel," *Journal of Communications and Networks*, vol. 14, no. 2, pp. 151–161, Apr. 2012.

[15] A. Sendonaris, E. Erkip, and B. Aazhang, "User cooperation diversity. part I. System description," *IEEE Trans. Commun.*, vol. 51, no. 11, pp. 1927–1938, Nov. 2003.

[16] N. Su, O. Kaya, S. Ulukus, and M. Koca, "Cooperative multiple access under energy harvesting constraints," in *IEEE GLOBECOM*, Dec. 2015.